Available online at www.sciencedirect.com
SCIENCE DIRECT
Colloids and Surfaces A: Physicochem. Eng. Aspects 270–271 (2005) 52–60
COLLOIDS AND SURFACES A
www.elsevier.com/locate/colsurfa

Influence of a new amphiphilic peptide with phospholipid monolayers at the air–water interface

Hiromichi Nakahara [a], Shohei Nakamura [a], Sannamu Lee [b], Gohsuke Sugihara [b], Osamu Shibata [a,*]

[a] *Division of Biointerfacial Science, Graduate school of Pharmaceutical Sciences, Kyushu University, 3-1-1 Maidashi, Higashi-ku, Fukuoka 812-8582, Japan*
[b] *Department of Chemistry, Faculty of Science, Fukuoka University, 8-19-1 Nanakuma, Johnan-ku, Fukuoka 814-0180, Japan*

Available online 11 July 2005

Abstract

Langmuir monolayer (surface pressure (π)–area (A), surface potential (ΔV)–area (A), and dipole moment ($\mu_\perp$)–area (A) isotherms) and fluorescence microscopy techniques were used to investigate a new-designed 18-mer amphiphilic α-helical peptide (Hel 13-5) which consists of 13 hydrophobic and 5 hydrophilic amino acid residues. We present here a study of the surface behavior of Hel 13-5 against dipalmitoylphosphatidylcholine (DPPC) and/or Egg-phosphatidylcholine (Egg-PC), which are major components in artificial pulmonary surfactant. A temperature dependence of pure DPPC and Hel 13-5 was examined using Langmuir isotherm techniques over the temperature range of 298.2–310.2 K. Basic interfacial behavior of Hel 13-5 was investigated by adding Hel 13-5 to pure DPPC and the DPPC/Egg-PC (1:1, mol:mol) mixture on a substrate solution of 0.02 M Tris buffer (pH 7.4) with 0.13 M NaCl at 298.2 K. The cyclic compression–expansion isotherms of these systems were obtained to confirm the spreading and respreading abilities of Hel 13-5. In addition, fluorescence microscopy measurements were carried out to understand the interactions of Hel 13-5 with pure DPPC or the DPPC/Egg-PC mixture. From the fluorescent images, the distinct differences between these systems were observed. Adding a small amount of Hel 13-5 to DPPC induced the "moth-eaten" disaggregation of liquid-condensed (LC) domains made of DPPC. On the other hand, the phenomenon that the LC domains were shrunk in size by adding a small amount of Hel 13-5 occurred for the there-component system (DPPC/Egg-PC/Hel 13-5).

Keywords: Pulmonary surfactant; Respiratory distress syndrome; Langmuir monolayer; π–A isotherm; ΔV–A isotherm; $\mu_\perp$–A isotherm; DPPC; Egg-PC; Hel 13-5; Fluorescence microscopy

1. Introduction

Pulmonary surfactant (PS) secreted by the alveolar type II cell is complex mixture of lipids and proteins. PS lining at the air/alveolar interface of the mammalian lung mainly contributes to maintaining the structural stability of the alveolus during respiration. This function in vivo reduces the surface tension down to almost zero on expiration, facilitating the work of breathing and preventing alveolar collapse at low volumes [1]. Deficiency of PS causes neonatal respiratory distress syndrome (NRDS) in premature infants, resulting in extremely high mortality rates.

PS consists of multiple lipids (∼90 wt.%) and four surfactant proteins (SP-A–SP-D; ∼10 wt.%). Although the compositions of PS are quite different among diverse species [2–5], it contains practically phospholipids (80–90 wt.%). Furthermore, the phospholipids largely include phosphatidylcholines (main component is dipalmitoylphosphatidylcholine, DPPC of ∼50%) in human PS. Pulmonary surfactant proteins play a decisive role as well, even though their content is less than 10 wt.% of the surfactant mass.

A single monolayer of the most abundant molecular species, DPPC, can reduce the surface tension down to almost zero under the excess compression beyond the collapse of the monolayer states. However, pure DPPC film does not sufficiently keep the surface tension low due to the space caused by a bulky head group of DPPC and is also sensible to mechanical disturbance and collapses irreversibly when compressed

* Corresponding author. Tel.: +81 92 642 6669; fax: +81 92 642 6669.
E-mail address: shibata@phar.kyushu-u.ac.jp (O. Shibata).
URL: http://kaimen.phar.kyushu-u.ac.jp/.

0927-7757/$ – see front matter © 2005 Elsevier B.V. All rights reserved.
doi:10.1016/j.colsurfa.2005.05.036

beyond the minimum surface tension [6]. In addition, it is very slow to adsorb from the aqueous suspension and to respread when compression is relieved. Hydrophobic proteins (SP-B and SP-C) concerned with interfacial functions can resolve these defects in native PS [2,7,8]. While, hydrophilic proteins (SP-A and SP-D) play an important role in the first line defense against inhaled pathogens [9]. Furthermore, SP-A regulates surfactant homeostasis [10–12]. Although hydrophobic proteins may collapse at relatively high surface tensions where the ejection of materials from the monolayer occurs, they facilitate the adsorption and spreading of surfactant molecules [13,14]. This specific phenomenon has been known as "squeeze-out" theory [15]. The theory describes that the fluidizing lipids are selectively removed from the interface on compression, leaving behind the monolayer enriched in lipids that possess abilities of lowering surface tension [16–18]. The "squeeze-out" theory includes an idealized immiscible interaction between the LC phase (rigid) and LE phase (fluid) of lipid components.

Pulmonary surfactant (PS) works in three-dimensional alveoli. However, Langmuir monolayer system characterized by two-dimensional surface films serves as a good model for biophysical studies of PS. At the air–liquid interface, direct visualization of lipid or lipid–protein monolayers doped with fluorescent probes and fluorescence microscopy (FM) measurement now provide the powerful information about structural transitions on dynamic compression [14,19–21].

Recently, we synthesized a de novo-designed 18-mer amphiphilic α-helical peptide (Hel 13-5), consisting of 13 hydrophobic and 5 hydrophilic amino acid residues [22]. In addition, we have already reported that Hel 13-5 could induce neutral liposomes to adopt long nanotubular structures and that the interaction of specific peptides with specific phospholipid mixtures could induce the membrane structures to resemble cellular organelles, such as Goldi apparatus [23–27]. Furthermore, we found that the size and shape of such nanotubes depend on lipid compositions [26]. Incidentally, Hel 13-5 (MW ∼2200) is considerably similar to SP-B (79 amino acid residues, MW ∼8700) and SP-C (35 amino acid residues, MW ∼4200) in terms of α-helical structure that is important for lipid–protein interactions in the monolayer state. These confirmations suggest that synthesized Hel 13-5 substitutes for native SP-B and SP-C to fulfill the pulmonary function at the alveolar liquid–protein interface.

In this study, the behavior of spread monolayers for multicomponent systems of new synthesized Hel 13-5 and pure DPPC or DPPC/Egg-PC (1:1, mol:mol) was investigated by surface pressure (π)–, surface potential (ΔV)–, surface dipole moment ($\mu_\perp$)–area (A) isotherms, and fluorescence microscopy (FM). DPPC is the main phospholipid in mammalian PS and the main surface-active constituent, too. In addition, two-component system (DPPC/Egg-PC) is applied to mimic the phosphatidylcholine components of the alveolar membranes [2–5]. Monolayers mainly spread on a 0.02 M Tris buffer (pH 7.4) with 0.13 M NaCl at 298.2 K were investigated at the air/water interface. The study was made on the temperature dependence of pure DPPC and Hel 13-5 in order to understand the monolayer stability, the solubility into aqueous subphase, and the structure change over the temperature range of 298.2–310.2 K. In addition, the cyclic compression–expansion isotherms, known as a hysteresis curve, of these two- or three-component systems were carried out to examine the spreading and respreading abilities of Hel 13-5.

2. Experimental

2.1. Materials

Hel 13-5 (MW 2203 Da) was synthesized by Fmoc strategy based on the solid phase technique starting from Fmoc-Leu-PEG-PS resin (0.1 m mol scale) with Perseptive 9050 automatic peptide synthesizer and purified by HPLC with reversed-phase column (20 mm × 250 mm, YMC C8) as described previously [22]. Dipalmitoyl phosphatidylcholine (DPPC, purity > 99%) and egg-phosphatidylcholine (Egg-PC, purity > 99%) were obtained from Avanti Polar Lipids Inc. (Birmingham, Alabama, USA). 3,6-bis(diethylamino)-9-(2-octadecyloxycarbonyl) phenyl chloride (R18) was obtained from Molecular Probes as a fluorescent probe. They were used without further purification or characterization. *n*-Hexane and ethanol (specially prepared reagent) used as spreading solvents were from Merck (Uvasol) and Nacalai Tesque, respectively. Tris (hydroxymethyl) aminomethane (Tris) and acetic acid (HAc) of guaranteed reagent grade for the preparation of a subphase were purchased from Nacalai Tesque. Sodium chloride (Nacalai Tesque) was roasted at 1023 K for 24 h to remove any surface-active organic impurities. We used two model surfactant lipids; pure DPPC [28] and DPPC:Egg-PC [23] (DPPC:Egg-PC = 1:1 by molar ratio).

2.2. Methods

2.2.1. Surface pressure–area isotherms

The surface pressure (π) of the monolayer was measured by using an automated home-made Wilhelmy balance, which was the same as that used in the previous studies [29]. The surface pressure balance (Mettler Toledo, AG-64) has a resolution of 0.01 mN m^{-1}. The pressure-measuring system was equipped with a filter paper (Whatman 541, periphery 4 cm). The trough was made from a Teflon-coated brass (area of 15 cm × 50 cm). The π–A isotherms were recorded over the temperature range from 298.2 to 310.2 K. The subphase and the ambient air temperature were precisely controlled by the thermostat and the clean room-grade ribbon heater, respectively. Solutions of DPPC (1.35 mM) and Egg-PC (1.35 mM) were prepared in *n*-hexane/ethanol (9/1, v/v), and that of Hel 13-5 was made in *n*-hexane/ethanol (4.5/5.5 v/v). The spreading solvent was allowed to evaporate for 15 min prior to compression. The monolayer was compressed at a speed of < 0.45 nm^2 molecule^{-1} min^{-1}.

In cyclic experiments, the proper films were compressed and expanded alternately through five cycles at a rate of 0.1–0.2 nm^2 $molecule^{-1}$ min^{-1}. The standard deviations for area and surface pressure measurements were ∼0.01 nm^2 and ∼0.1 mN m^{-1}, respectively. The subphase pH was controlled to be pH 7.4 with a 0.02 M Tris (hydroxymethyl) aminomethane (Tris) buffer and with adequate acetic acid (HAc). All monolayers were studied on the buffer subphase (0.02 M Tris, pH 7.4) with 0.13 M NaCl. Throughout these studies, the water used was thrice-distilled (surface tension of 72.7 mN m^{-1} at 293 K and electrical resistivity of 18 MΩ cm).

2.2.2. Surface potential measurements

The surface potential (ΔV) was simultaneously recorded, while the monolayer was compressed. It was monitored by using an ionizing ^{241}Am electrode at 1–2 mm above the interface, while a reference electrode was dipped in the subphase. The ionizing ^{241}Am electrode is warmed by the clean room-grade ribbon heater at 303.2–310.2 K in order to prevent it from forming dew drops on the surface of the electrode. The standard deviation for surface potential measurements was ∼5 mV. The other experimental conditions were the same as described in previous papers [29–32].

2.2.3. Fluorescence microscopy

Fluorescence microscopy (U.S.I. System BM-1000) observation and the compression isotherm measurement were carried out simultaneously. The spreading solution was prepared as the mixed solution doped with 1 mol% fluorescence probe. A 300 W Xenon lamp (XL 300, Pneum) was used for excitation of the probe. Excitation and emission wavelengths were selected as 560 and 581 nm, respectively, by an appropriate beam splitter/filter combination (Mitutoyo band path filter, 546 nm; cut filter Olympus, 590 nm). The monolayer was observed by using a 20-hold magnification of long-distance objective lens (Mitutoyo f = 200/focal length (20 mm)). Fluorescent micrographs were recorded with a video camera (757 JAI ICCD camera, Denmark) connected to the microscopy and stored directly into computer memory via an online image processor (Vaio PCV-R53 Sony: Video Capture Soft). The entire optical set-up was placed on an active vibration isolation unit (Model-AY-1812, Visolator, Japan). The image processing and analysis were carried out by using the software, Scion Image Beta 4.02 for Windows (Scion Corporation).

3. Results and discussion

3.1. Temperature dependence of pure DPPC and Hel 13-5

The amphiphilic α-helical peptide KLLKLLLKL-WLKLLKLLL (Hel 13-5) consists of 13 hydrophobic residues (12 Leu and 1 Trp) and 5 hydrophilic residues (5 Lys). The hydrophobic–hydrophilic balance (HHB) was estimated both theoretically from the calculated hydrophobicity value (or the magnitude of hydrophobic faces) and experimentally from the retention times in reverse phase high-performance liquid chromatography (RP-HPLC). For this modulation (hydrophobicity of Hel 13-5 is 0.07), it is supposed that Hel 13-5 structurally mimics SP-B and SP-C at the alveolar air/liquid interface. Furthermore, Hel 13-5 forms the amphiphilic structure with a 260° hydrophobic sector region as shown in the helical wheel representation (Fig. 1), indicating that the hydrophobic part and the hydrophilic one are completely separated. Our general objective being to investigate the potential benefits of Hel 13-5 to facilitate DPPC respreading, buffer solution (0.02 M Tris, pH 7.4) with 0.13 M NaCl was chosen as the subphase in order to mimic a biomembrane-like environment. This condition is very popular to many researchers [33-36].

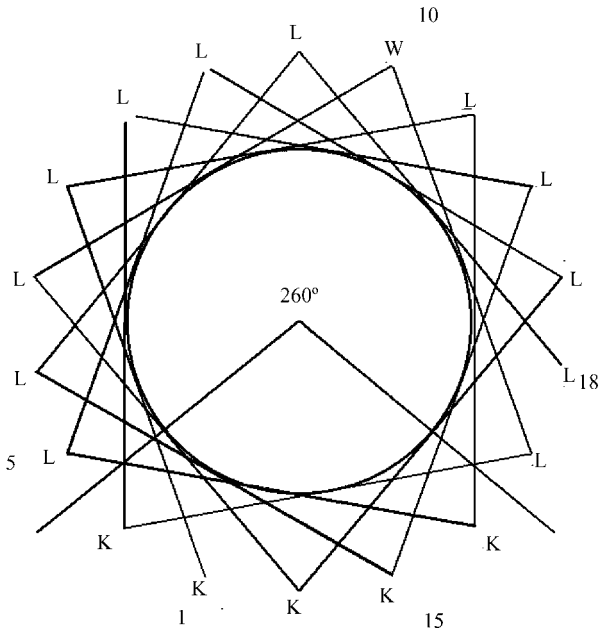

Fig. 1. Helical wheel representation of Hel 13-5.

Fig. 2A and B shows some π–A, ΔV–A, and $\mu_\perp$–A isotherms of monolayers at 298.2, 303.2, and 310.2 K for pure DPPC and Hel 13-5, respectively. The vertical component of the surface dipole moment, $\mu_\perp$, was obtained by calculation by the Helmholtz equation:

$$\Delta V = \frac{\mu_\perp}{\varepsilon_0 \varepsilon A} \quad (1)$$

where ε_0 is the permittivity of a vacuum and ε is the mean permittivity of the monolayer (which is assumed to be 1). Although the transition pressure (π^{eq}) might be determined only from the π–A isotherms, π^{eq} could be more precisely determined by using ΔV–A and $\mu_\perp$–A isotherms, since ΔV is more sensitive than π. This can be also applied to the collapse pressure (π^c), because ΔV–A isotherms become

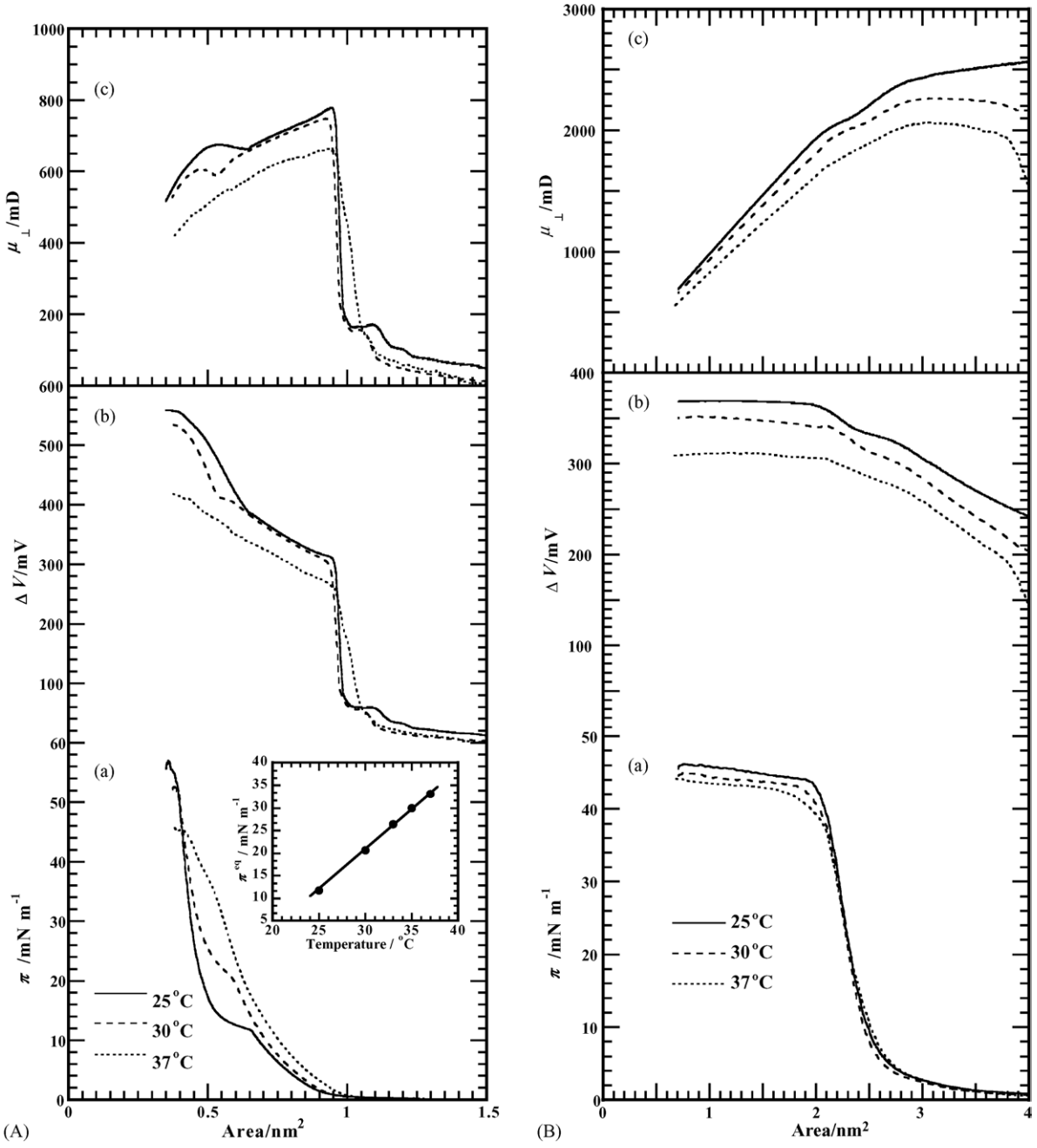

Fig. 2. (a) Surface pressure (π)–area (A) isotherms, (b) surface potential (ΔV)–A isotherms, and (c) surface dipole moment ($\mu_\perp$)–A isotherms of pure DPPC monolayer on 0.15 M NaCl and Hel 13-5 monolayer on a 0.02 M Tris buffer solution (pH 7.4) with 0.13 M NaCl at different temperatures (indicated). (A) Pure DPPC and (B) Hel 13-5 monolayers. The inserted figure shows the transition pressure (π^{eq})–temperature isotherm.

the flat lines above the collapse pressure. In Fig. 2A, pure DPPC at 298.2 K on 0.15 M NaCl had the transition pressure ($\pi^{eq} = 11.3\,mN\,m^{-1}$ at $0.65\,nm^2$) and the collapse pressure ($\pi^{c} = 55.4\,mN\,m^{-1}$ at $0.34\,nm^2$), showing the good agreement with those in previous papers [29,32]. The present parameter values of DPPC at 303.2–310.2 K are in good agreement with those by many researchers [37–39]. The inserted figure in Fig. 2A represents the π^{eq} change with temperature. For the transition pressure, π^{eq} linearly increased with increasing temperature. The phase transition surface pressure (π^{eq}) at given temperature is a characteristic quantity for a given lipid in a monolayer on a given subphase. For DPPC on pure water, π^{eq} is $\sim$4 mN m^{-1} at 293.2 K and shifts by $\partial\pi^{eq}/\partial T = 1.5\,mN\,m^{-1}\,K^{-1}$ until a critical point is reached at $T_t = 316.2$ K [40]. On 0.02 M Tris buffer (pH7.4) with 0.13 M NaCl, π^{eq} of DPPC was $\sim$11.5 mN m^{-1} at 298.2 K. For DPPC above subphase condition, π^{eq} is $\sim$11.5 mNm^{-1} at 298.2 K and shifts by $\partial\pi^{eq}/\partial T = 1.75\,mN\,m^{-1}\,K^{-1}$ until

Table 1
Temperature dependence of Langmuir isotherm data for pure DPPC and Hel 13-5[a]

Temperature (°C)	A_0 (nm^2)	π^c (mN m^{-1})	ΔV_{max} (mV)
DPPC			
25	0.50	55.2	552.4
30	0.55	52.1	532.8
33	0.57	50.4	505.6
35	0.64	48.8	482.9
37	0.86	44.9	410.5
Hel 13-5			
25	2.54	42.2	369.3
30	2.54	39.4	350.9
33	2.54	38.7	341.1
35	2.56	38.9	319.9
37	2.58	38.5	311.5

[a] A_0, liming (extrapolated) area; π^c, collapse pressure; ΔV_{max}, ΔV at maximum value.

the temperature is 310.2 K. So ionic strength, the subphase and ambient air temperature control have an effect on π^{eq}.

On the other hand, π^c shifted to lower values with increasing temperature, indicating that DPPC monolayer becomes more fluidized as temperature rises. In other words, rising temperature facilitates DPPC molecules to form a liquid-expanded (LE) phase. The isotherm data of DPPC, the limiting area (A_0), the collapse pressure (π^c), and the maximum of surface potential (ΔV_{max}), confirm this phenomenon (see Table 1).

In the case of pure Hel 13-5 (Fig. 2B), Hel 13-5 dose not possess the first-order phase transition from a liquid expanded (LE) to a liquid condensed (LC) phase at examined temperatures contrary to the case of pure DPPC. Table 1 shows that Hel 13-5 monolayer is not much influenced by temperature changes in comparison to DPPC. Namely, Hel 13-5 monolayer is quite stable against the temperature change at the air–water interface and has the low solubility into aqueous subphase. However, this does not mean that the desorption of Hel 13-5 monolayer into the subphase does not occur. We will discuss about this later.

3.2. π–A, ΔV–A, and $\mu_\perp$–A isotherms of two- or three-component systems

After the examination of one component system, we move to the two- or three-component systems especially at 298.2 K, because the LE/LC coexistence region in the one-component systems comes to disappear at high temperatures. So, the present experimental condition was designed to understand the interfacial behavior of two-component systems by observing and analyzing their immiscibility phenomenon; the coexistence of both fluid compositions (LE phase) and non-fluid ones (LC phase) and their interaction. Typical isotherms of Hel 13-5 containing pure DPPC or two phosphatidylcholines (PCs: DPPC:Egg-PC = 1:1, mol:mol) were studied in order to assess the effect of Hel 13-5 as a component for pulmonary surfactant lipid and the potential use of Hel 13-5 as a pulmonary surfactant protein analog. For the above purposes, the π–A, ΔV–A, and $\mu_\perp$–A isotherms of the DPPC/Hel 13-5 and PCs/Hel 13-5 multi-component systems were measured for various Hel 13-5 mole fractions ($X_{Hel\ 13\text{-}5}$) on 0.02 M Tris buffer (pH 7.4) with 0.13 M NaCl at 298.2 K. These results are shown in Fig. 3. Because the pulmonary surfactant contains only ∼10 wt.% surfactant proteins, the attention was focused on the smaller molar contents of Hel 13-5 as seen in Fig. 3A and B.

For DPPC/Hel 13-5 mixture (Fig. 3A), all π–A isotherms (except for pure DPPC) had two clear kink points at 11.5–19.0 mN m^{-1} and at ∼42 mN m^{-1}; the kink points are indicated by the arrows in $X_{Hel\ 13\text{-}5} = 0.3$. The first kink point at lower surface pressure and the second one at higher surface pressure indicate the first-order LE/LC transition pressure and the collapse pressure of Hel 13-5, respectively. The transition points of all the π–A isotherms increased from 11.5 to 19.0 mN m^{-1} and became less clear with increasing $X_{Hel\ 13\text{-}5}$, implying that Hel 13-5 attractively interacted with DPPC at low surface pressure in the two-component monolayer. The second kink points appeared at ∼42 mN m^{-1}, π^c of pure Hel 13-5 monolayer, and the second plateaus are broadened with increasing $X_{Hel\ 13\text{-}5}$. It is quite interesting that the second kink points appeared at the same surface pressure (∼42 mN m^{-1}) independent of their compositions. This observation implies that Hel 13-5 repulsively interacts with DPPC at high surface pressure with the two components immiscible. Only the Hel 13-5 molecules begin to be squeezed out of the DPPC/Hel 13-5 two-component system at ∼42 mN m^{-1} and then the squeezing-out is gradually facilitated upon further compression. Finally most components would be DPPC at the air–water interface around 55 mN m^{-1}, π^c of pure DPPC monolayer.

In the PCs/Hel 13-5 mixture (Fig. 3B), all π–A isotherms (except for PCs) had only the second plateau corresponding to π^c of Hel 13-5 monolayer. Only PCs possessed a LE/LC coexistence state which is indicated by an arrow. Like the DPPC/Hel 13-5 system above, the second plateaus were widened as $X_{Hel\ 13\text{-}5}$ increased and the second kink points (∼42 mN m^{-1}) were independent of their compositions. By the way, the PCs monolayer and PCs/Hel 13-5 mixed monolayer ($0 < X_{Hel\ 13\text{-}5} \leq 0.3$) formed stable films up to ∼43 and ∼48 mN m^{-1}, respectively. Egg-PC is a mixture of PC composed of various acyl chain lengths with the same PC head group. So, it is expected that Hel 13-5 together with fluid (unsaturated) components in Egg-PC is squeezed out of the PCs/Hel 13-5 monolayers at ∼42 mN m^{-1}, and more rigid (saturated) components in Egg-PC are refined at the air–water interface. So, π^c of PCs/Hel 13-5 mixed monolayer ($X_{Hel\ 13\text{-}5} = 0.1 \sim 0.3$) became larger than that of only PCs without Hel 13-5. These specialties, the squeezing-out phenomenon and the collapse pressure increase of the second kink points, were also observed in the systems of SP-B and SP-C [41,42]. These similarities with native SP-B and SP-C support the possibility of Hel 13-5 as the substitute for them.

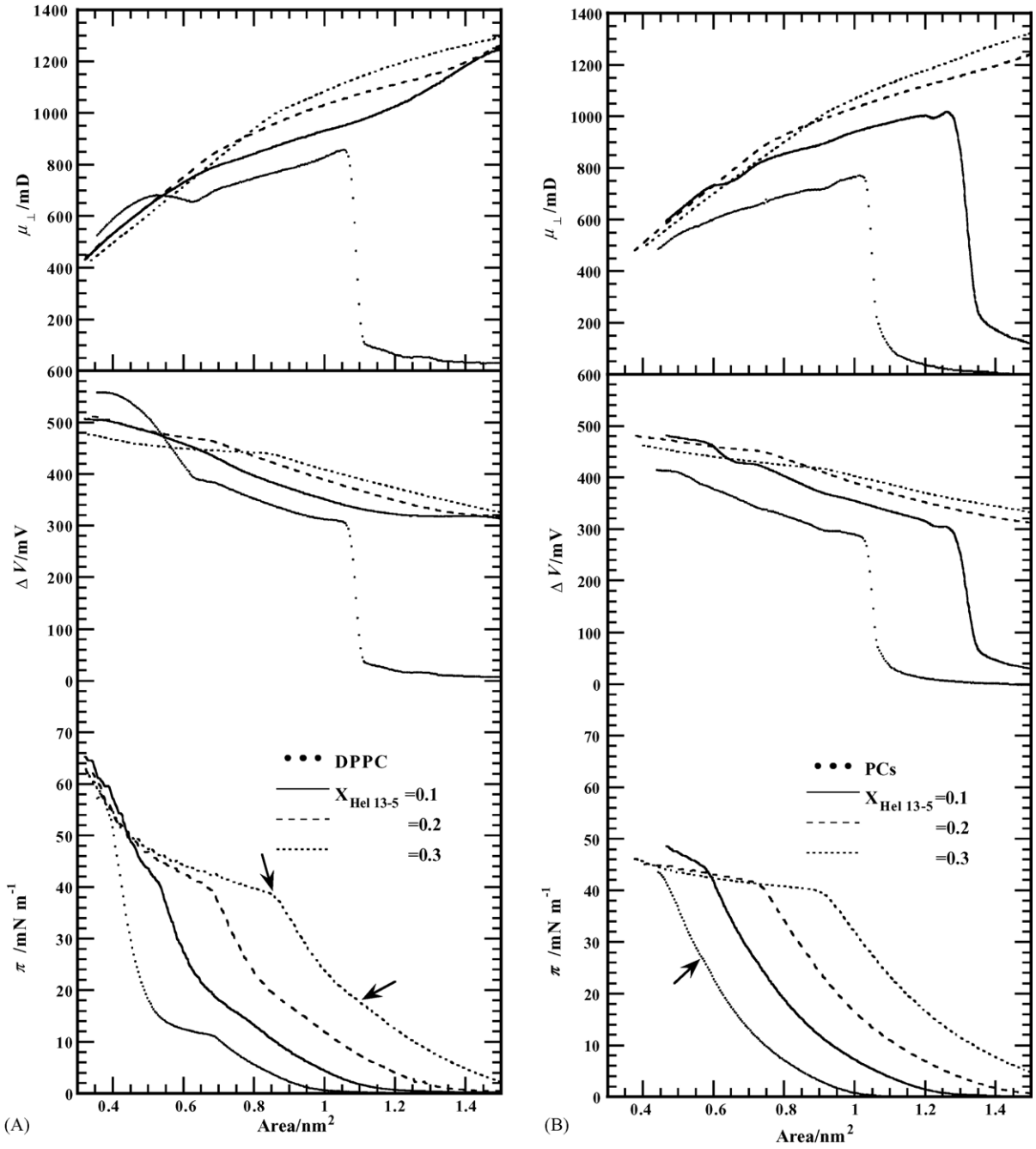

Fig. 3. Surface pressure (π)–area (A) isotherms, surface potential (ΔV)–A isotherms, and surface dipole moment ($\mu_\perp$)–A isotherms of the DPPC/Hel 13-5 and PCs (DPPC:Egg-PC/1:1/mol:mol)/Hel 13-5 mixtures on a 0.02 M Tris buffer solution (pH 7.4) with 0.13 M NaCl at 298.2 K. (A) DPPC/Hel 13-5 and (B) PCs/Hel 13-5 systems.

3.3. Fluorescence microscopy

Fig. 4 and Fig. 5 show FM images of two systems (DPPC/Hel 13-5 and PCs/Hel 13-5) at surface pressures at 15 and 30 mN m^{-1}, respectively. An upper right monochrome domain in each FM image corresponds to the domain indicated by a white arrow. Generally, it is widely accepted that the fluorescent probe is selectively dissolved in the LE phase, not dissolving in the LC phase. Therefore, FM images can be observed in the LE/LC coexistence region. The fluorescent images confirmed the coexistence of two phases in pure DPPC films (Fig. 4a), where the bright regions and dark domains indicated the LE and the LC phase, respectively. LC domains grew more with increasing surface pressure and finally FM images became homogenous black (or the complete LC phase) up to the collapse pressure [29,32]. The FM images in Fig. 4b and c also showed the LE/LC coexistence states; that is, dark domains reflect the LC domains

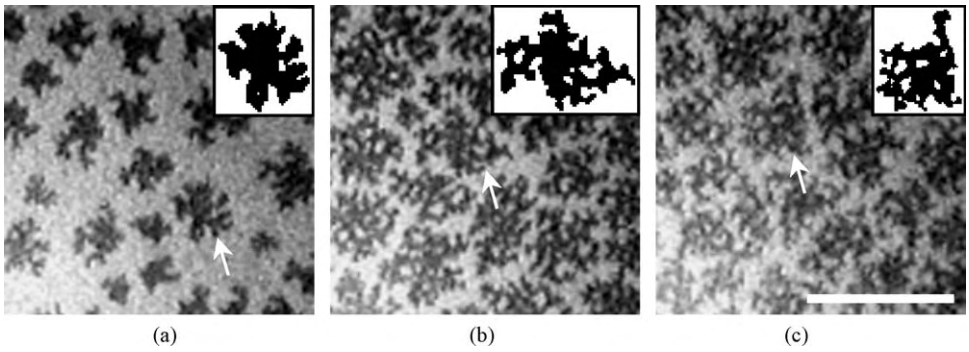

Fig. 4. FM images of the DPPC/Hel 13-5 system at 15 mN m^{-1}. The domain indicated by a white arrow is converted into the monochrome domain, which is inserted in an upper right. The monolayers contain 1 mol% fluorescent probe (R18). The scale bar in the lower right represents 100 μm; (a) pure DPPC, (b) $X_{\text{Hel 13-5}} = 0.005$, and (c) $X_{\text{Hel 13-5}} = 0.025$.

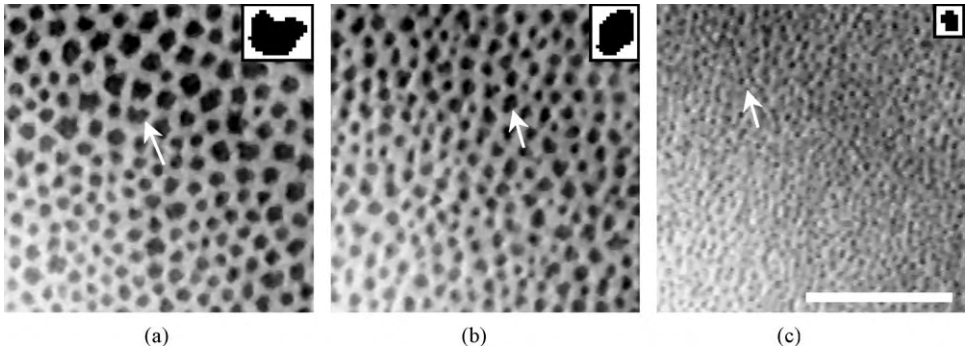

Fig. 5. FM images of the PC's (DPPC:Egg-PC/0.75:0.25/mol:mol)/Hel 13-5 mixture at 30 mN m^{-1}. The domain indicated by a white arrow is converted into the monochrome domain, which is inserted in an upper right. The monolayers contain 1 mol% fluorescent probe (R18). The scale bar in the lower right represents 100 μm; (a) PC's, (b) $X_{\text{Hel 13-5}} = 0.005$, and (c) $X_{\text{Hel 13–5}} = 0.025$.

of DPPC and bright regions do the LE phases of DPPC and Hel 13-5. Each LC domain of all molar fractions grew in area with adding Hel 13-5 to DPPC. When the films were compressed further, they became homogeneous black images consisting mostly of the LC phase up to the collapse pressure (the data are not shown). It is interesting that the addition of a small amount of Hel 13-5 to DPPC induces the "moth-eaten" disaggregation of LC domains made of pure DPPC. This "moth-eaten" disaggregation was observed, only when a small amount of Hel 13-5 was added to DPPC. Considering the isotherm data and FM images, it is suggested that the miscible interaction between Hel 13-5 and DPPC at the low surface pressure induces the penetration of Hel 13-5 into LC domains derived from DPPC (Fig. 4b and c).

In the FM image of only PCs, quite a small LC domain was observed (the data are not shown). For better understanding of the LE/LC phase transition of the PCs/Hel 13-5 system, more DPPC was added to PCs. Now, we define the new phosphatidylcholine mixture (PCs': DPPC:Egg-PC = 0.75:0.25, mol:mol). Fig. 5a indicates the LE/LC coexistence state of only PCs' at 30 mN m^{-1}. This coexistence phases were similarly observed beyond 30 mN m^{-1} up to the collapse pressure (the data is not shown). FM images of the PCs'/Hel 13-5 system at 30 mN m^{-1} are shown in Fig. 5b and c. The PCs'/Hel 13-5 systems indicated the LE/LC coexistence states. LE/LC coexistence states continued from 30 mN m^{-1} up to the collapse pressures (the data are not shown). It is notable that the addition of a small amount of Hel 13-5 to PCs' induced such interaction as LC domains shrank in size contrary to the DPPC/Hel 13-5 system. Considering these results in Fig. 5, the similar behavior might be also observed for the PCs/Hel 13-5 system. These FM images in Figs. 4 and 5 suggest that the various interactions between phosphatidylcholines and Hel 13-5 result from the different effects of Hel 13-5 on fluid (LE) components or on non-fluid (LC) ones of phosphatidylcholine groups.

3.4. Cyclic compression–expansion isotherms

Hysteresis curves in the two systems of DPPC/Hel 13-5 ($X_{\text{Hel 13-5}} = 0.1$) and PCs/Hel 13-5 ($X_{\text{Hel 13-5}} = 0.2$) are shown in Fig. 6. These two mixtures were compressed up to the surface pressures of 55 mN m^{-1} (DPPC/Hel 13-5) and 46 mN m^{-1} (PCs/Hel 13-5) and then expanded to the corresponding starting area. This process was repeated five times. During the cycling, any loss materials from the surface were not observed. For the DPPC/Hel 13-5 system (Fig. 6a), the second kink point where Hel 13-5 was desorbed from the interface clearly appeared in spite of repeated cycling pro-

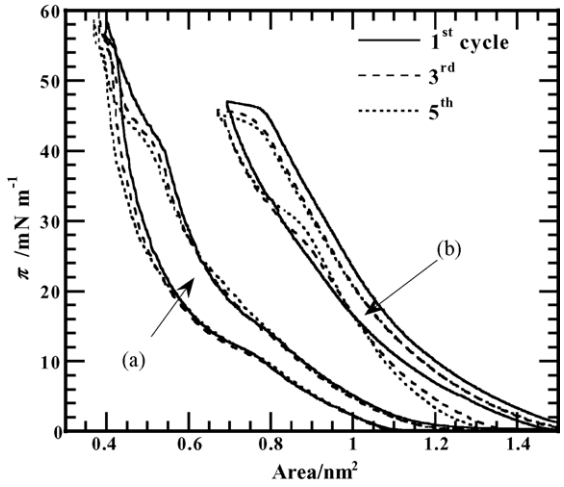

Fig. 6. The cyclic compression–expansion isotherms of the (a) DPPC/Hel 13-5 ($X_{\text{Hel 13-5}} = 0.1$) and (b) PCs(DPPC:Egg-PC/1:1/mol:mol)/Hel 13-5 ($X_{\text{Hel 13-5}} = 0.2$) mixtures on a 0.02 M Tris buffer solution (pH 7.4) with 0.13 M NaCl at 298.2 K. Compression–expansion cycle was done five times at compression rate of 0.1–0.2 nm^2 molecule^{-1} min^{-1}.

cesses. In addition, the first cycling π–A isotherm almost coincided with the third and fifth cycle ones. This behavior indicates that the adsorption–desorption process of Hel 13-5 is reversible. On the other hand in Fig. 6b, the second kink shoulder appeared without getting unclear, as is the same for Fig. 6a. Both Fig. 6a and b support that Hel 13-5 can accelerate the spreading of the phosphatidylcholines and induce the good respreading. In addition, these hysteresis curves nicely resemble those of the DPPC/native SP-B or SP-C mixtures [43,44], supporting the high possibilities of Hel 13-5 as alternatives for SP-B and SP-C.

4. Conclusions

Langmuir isotherms of the multi-component systems (DPPC/Hel 13-5 and PCs (=DPPC:Egg-PC/1:1/mol:mol) /Hel 13-5) supported the squeeze-out phenomenon of Hel 13-5 from these mixtures. In addition, FM measurements in the DPPC/Hel 13-5 system demonstrated the “moth-eaten” disaggregation of LC domain derived from DPPC by adding a small amount of Hel 13-5. On the other hand, the PCs/Hel 13-5 mixture showed that LC domains shrank in size with increasing $X_{\text{Hel 13-5}}$. Finally, compression–expansion curves of these systems implied that Hel 13-5 facilitated the spreading of phosphatidylcholines and induced the good respreading of these mixtures. Judging from these analyses, Hel 13-5 (or the amphiphilic α-helical peptide) has ability similar to SP-B and SP-C. Hel 13-5 can be synthesized at a lower cost in comparison with KL_4, a cationic and hydrophobic peptide (21-mer α-helical peptide) used as a substitute for SP-B [34,45–47]. Furthermore, Hel 13-5 has no risk of disease transmissions from animals in contrast to native SP-B and SP-C.

Acknowledgments

This work was partially supported by Grant-in-aid for Scientific Research from the Kieikai Foundation (Japan), which is greatly appreciated.

References

[1] S. Schürch, J. Goerke, J.A. Clements, Proc. Natl. Acad. Sci. USA 73 (1976) 4698.
[2] R. Veldhuizen, K. Nag, S. Orgeig, F. Possmayer, Biochim. Biophys. Acta 1408 (1998) 90.
[3] C.S. Gross, P.J. Simms, R.W. Towne, R.E. Miller, J. Chromatogr. B 744 (2000) 407.
[4] R.H. Notter, Z. Wang, E.A. Egan, B.A. Holm, Chem. Phys. Lipids 114 (2002) 21.
[5] S.-H. Yu, F. Possmayer, J. Lipid Res. 44 (2003) 621.
[6] S. Schürch, F.H.Y. Green, H. Bachofen, Biochim. Biophys. Acta 1408 (1998) 180.
[7] S. Hawgood, M. Derrick, F. Poulain, Biochim. Biophys. Acta 1408 (1998) 150.
[8] J. Johansson, Biochim. Biophys. Acta 1408 (1998) 161.
[9] K. Miyamura, E.A.L. Leonora, L. Jinhua, J. Hopkin, A.L. Bernal, K.B.M. Reid, Biochem. J. 300 (1994) 237.
[10] J.R. Wright, R.E. Wager, S. Hawgood, L. Dobbs, J.A. Clements, J. Biol. Chem. 262 (1987) 2888.
[11] W.R. Rice, G.F. Ross, F.M. Singleton, S. Dingle, J.A. Whitsett, J. Appl. Physiol. 63 (1987) 692.
[12] L.G. Dobbs, J.R. Wright, S. Hawgood, R. Gonzalez, K. Venstrom, J. Nellenbogen, Proc. Natl. Acad. Sci. USA 84 (1987) 1010.
[13] M.M. Lipp, K.Y.C. Lee, D.Y. Takamoto, J.A. Zasadzinski, A.J. Waring, Phys. Rev. Lett. 81 (1998) 1650.
[14] K. Nag, J. Perez-Gil, M.L.F. Ruano, L.A.D. Worthman, J. Stewart, Biophys. J. 74 (1998) 2983.
[15] J. Goerke, Biochim. Biophys. Acta 1408 (1998) 79.
[16] J. Egberts, H. Sloot, A. Mazure, Biochim. Biophys. Acta 1002 (1989) 109.
[17] B. Pastrana-Rios, C.R. Flach, W. Brauner, A.J. Mautone, R. Mendelsohn, Biochemistry 33 (1994) 5121.
[18] A. Boonman, F.H.J. Machiels, A.F.M. Snik, J. Egberts, J. Colloid Interf. Sci. 120 (1987) 456.
[19] B.M. Discher, K.M. Maloney, D.W. Grainger, C.A. Sousa, S.B. Hall, Biochemistry 38 (1999) 374.
[20] B. Piknova, W.R. Schief, V. Vogel, B.M. Discher, S.B. Hall, Biophys. J. 81 (2001) 2172.
[21] D. Knebel, M. Sieber, R. Reichelt, H.-J. Galla, M. Amrein, Biophys. J. 73 (2002) 547.
[22] T. Kiyota, S. Lee, G. Sugihara, Biochemistry 35 (1996) 13196.
[23] N. Ohmori, T. Niidome, T. Kiyota, S. Lee, G. Sugihara, A. Wada, T. Hirayama, H. Aoyagi, Biochem. Biophys. Res. Commun. 245 (1998) 259.
[24] A. Kitamura, T. Kiyota, S. Lee, G. Sugihara, Bull. Chem. Soc., Jpn. 71 (1998) 1151.
[25] A. Kitamura, T. Kiyota, M. Tomohiro, A. Umeda, S. Lee, T. Inoue, G. Sugihara, Biophys. J. 76 (1999) 1457.
[26] S. Lee, T. Furuya, T. Kiyota, N. Takami, K. Murata, Y. Niidome, D.E. Bredesen, H.M. Ellerby, G. Sugihara, J. Biol. Chem. 276 (2001) 41224.
[27] T. Furuya, T. Kiyota, S. Lee, T. Inoue, G. Sugihara, A. Logvinova, P. Goldsmith, H.M. Ellerby, Biophys. J. 84 (2003) 1950.
[28] M.E. Avery, J. Mead, Am. J. Dis. Child. 97 (1959) 517.
[29] H.M. Courrier, T.F. Vandamme, M.P. Krafft, S. Nakamura, O. Shibata, Colloid Surf. A 215 (2003) 33.
[30] O. Shibata, M.P. Krafft, Langmuir 16 (2000) 10281.

[31] M. Rusdi, Y. Moroi, S. Nakamura, O. Shibata, Y. Abe, T. Takahashi, J. Colloid Interf. Sci. 243 (2001) 370.
[32] T. Hiranita, S. Nakamura, M. Kawachi, H.M. Courrier, T.F. Vandamme, M.P. Krafft, O. Shibata, J. Colloid Interf. Sci. 265 (2003) 83.
[33] M.M. Lipp, K.Y.C. Lee, A. Waring, J.A. Zasadzinski, Biophys. J. 72 (1997) 2783.
[34] J. Ma, S. Koppenol, H. Yu, G. Zografi, Biophys. J. 74 (1998) 1899.
[35] S. Koppenol, F.H.C. Tsao, H. Yu, G. Zografi, Biochim. Biophys. Acta 1369 (1998) 221.
[36] B.N. Flanders, S.A. Vickery, R.C. Dunn, J. Phys. Chem. B 106 (2002) 3530.
[37] T.-H. Chou, C.-H. Chang, Colloids Surf. B 17 (2000) 71.
[38] S.A. Maskarinec, K.Y.C. Lee, Langmuir 19 (2003) 1809.
[39] K.-B. Chen, C.-H. Chang, Y.-M. Yang, J.-R. Maa, Colloids Surf. A 170 (2000) 199.
[40] O. Albrecht, H. Gruler, E. Sackmann, J. Phys. France 39 (1978) 301.
[41] D.Y. Takamoto, M.M. Lipp, A.V. Nahmen, K.Y.C. Lee, A. Waring, J.A. Zasadzinski, Biophys. J. 81 (2001) 153.
[42] R.V. Diemel, M.M.E. Snel, A.J. Waring, F.J. Walther, L.M.G.V. Golde, G. Putz, H.P. Haagsman, J.J. Batenburg, J. Biol. Chem. 277 (2002) 21179.
[43] R. Wüstneck, N. Wüstneck, B. Moser, U. Pison, Langmuir 18 (2002) 1125.
[44] N. Wüstneck, R. Wüstneck, V.B. Fainerman, R. Miller, U. Pison, Colloids Surf. B 21 (2001) 191.
[45] C.G. Cochrane, S.D. Revak, T.A. Merritt, G.P. Heldt, M. Hallman, M.D. Cunningham, D. Easa, A. Pramanik, D.K. Edwards, M.S. Alberts, Am. J. Respir. Crit. Care Med. 153 (1996) 404.
[46] S.D. Revak, T.A. Merritt, C.G. Cochrane, G.P. Heldt, M.S. Alberts, D.W. Anderson, A. Kheiter, Pediatr. Res. 39 (1996) 715.
[47] P. Cai, C.R. Flach, R. Mendelsohn, Biochemistry 42 (2003) 9446.